IJISEM
INTERNATIONAL JOURNAL OF INNOVATIONS IN SCIENCE ENGINEERING AND MANAGEMENT

International Journal of Innovations In Science Engineering And Management

OPEN ACCESS

Volume: 4

Issue: 2

Month: May

Year: 2025

ISSN: 2583-7117

Published: 26.04.2025

Citation:

Md. Ahsan Alam, Prof. Pankaj Shrivastava, Dr. B. Suresh "Optimization of Heat Transfer through Baffles and Various Velocity of Cold and Hot Fluid in Shell and Tube Heat Exchanger" International Journal of Innovations in Science Engineering and Management, vol. 4, no. 2, 2025, pp. 186–195.

DOI:

10.69968/ijisem.2025v4i2186-195

Optimization of Heat Transfer through Baffles and Various Velocity of Cold and Hot Fluid in Shell and Tube Heat Exchanger

Md. Ahsan Alam[1], Prof. Pankaj Shrivastava[2], Dr. B. Suresh[3]

[1]Research Scholar, Department of Mechanical Engineering, Corporate Institute Of Science & Technology, Bhopal.
[2]Asst Prof., Department of Mechanical Engineering, Corporate Institute Of Science & Technology, Bhopal.
[3]Prof. & HOD, Department of Mechanical Engineering, Corporate Institute Of Science & Technology, Bhopal

Abstract

The present work investigates the influence of different baffle structure variations on the outlet temperature of "shell-and-tube heat exchangers" when used as waste heat recovery systems. The remaining thermal energy from liquid heated to 65 °C was reclaimed by passing water at 10 °C via a network of tubes at the entrance. Various mass flow rates of 0.5, 0.3, and 0.2 kg/s were used to circulate water through the shell inlet, while 0.2, 0.15, and 0.1 kg/s were used in the tube inlet. In this study investigate the various combination of mass flow rate of both shell inlet and outlet. A rigorous three-dimensional computational investigation was performed using ANSYS-Fluent under steady-state circumstances. The adoption of the credible k-epsilon turbulence model was motivated by the possibility of transitioning from laminar flow to turbulence. The temperatures, pressure drop, and velocity, for all the cases were compared at both outlet and along the length of STHXs. Flow visualisation was achieved through the presentation of temperature contours, pressure contours, and velocity streamlines. Upon comparing the simulation results of the various STHXs, it was discovered that case 5 has the maximum temperature rise at the tube side, which is 292.226 K.

Keywords; Baffle, mass flow rate, velocity streamline, shell and tube heat exchanger (STHXs), waste heat recovery system.

INTRODUCTION

Heat exchangers are employed for the purpose of facilitating the transfer of thermal energy from one medium to another. The media in question can exist in a gaseous, liquid, or hybrid state [1]. The media can be physically divided by a solid barrier to avoid intermingling, or it can be in direct access to each other [2]. Heat exchangers are essential components that are necessary in order to fulfil the thermal demands of a given process, either by providing heating or cooling. A furnace or steam boiler is the typical source of direct heat input to the system [3]. So, if the heat transmission at the exchangers is inefficient, the boiler or steam will have to work harder [4]. Heat exchangers have the potential to enhance the energy efficiency of a system by facilitating the transfer of heat from systems where it is surplus to requirements to other systems where it may be effectively utilized [5]. In order to move heat from one process stream to another or from one process stream to a utility stream, heat exchangers are a typical piece of equipment. Both hot and cold utility streams are possible [6].

When discussing heat exchangers, the term "flow configuration" may be used to describe the relative orientations of the fluids moving through the device. Heat exchangers typically use one of four main flow configurations [2]. The fluids in a concurrent flow heat exchanger travel in the same direction and parallel to one another; this design is also known as a parallel flow heat exchanger [7].

The maximum thermal homogeneity across the heat exchanger's walls is achieved with this layout, although the efficiency is usually lower than with a counter flow setup [8]. The fluids of a "countercurrent flow heat exchanger" (or simply a counter flow heat exchanger) travel in the same direction but in opposing directions, creating an antiparallel flow [9]. Due to its ability to provide the most amount of heat transfer between fluids and thus, the largest temperature change, the counter flow configuration is often the most efficient flow design [10].

Fluids move in opposite directions in crossflow heat exchangers. In terms of efficiency, heat exchangers that use this flow arrangement are in the middle of the pack, somewhere between cocurrent and countercurrent [11]. Heat exchangers with a hybrid flow arrangement combine features of the two types of flows described above. A single heat exchanger, for instance, may make use of many flow passages and configurations (such as crossflow and counterflow) all at once [12]. When working with applications that have space, financial, or temperature and pressure constraints, these heat exchangers are usually the way to go [13].

"Shell and tube heat exchangers" consist of a bundle of tubes set within a cylindrical shell. A double pipe heat exchanger's inner pipe serves as a conductive barrier, much like the one mentioned before [14]. On one side, the tube carries the processed fluid, while on the other, the utility fluid is guided by the shell. When the fluids being heated or cooled have high flows, temperatures, and pressures, "shell and tube heat exchangers" are the way to go [15]. In order to enhance operational efficiency, it is possible to devise systems that incorporate numerous passes, hence facilitating repeated contact between two fluids [16].

In many waste heat recovery systems, customized heat exchangers are designed and operated to meet specific heat recovery needs. However, this study seeks to meet the demand of recovering waste heat from an operation that releases hot wastewater into the environment at a temperature of 65ºC. The investigation focuses on enhancing the performance of STHXs as prospective waste heat recovery systems that would effectively recover the waste heat for useful and productive services. Therefore, investigate the increasing the baffle in STHXs to maximize the performance. In addition, three different mass flow rate consider for both shell and tube inlet to investigate in terms of temperature, pressure, and velocity of the both hot and cold fluid.

RESEARCH AND METHODOLOGY

Governing equation

The following is a possible form for the governing equations:

Continuity equation.

$$\nabla . (\rho V) = 0$$

Momentum equation

- **x- direction;**

$$\nabla . (\rho u V) = -\frac{\partial p}{\partial x} + \left(\frac{\partial \tau_{xx}}{\partial x} + \frac{\partial \tau_{yx}}{\partial y} + \frac{\partial \tau_{zx}}{\partial z} \right)$$

- **y- direction;**

$$\nabla . (\rho v V) = -\frac{\partial p}{\partial y} + \left(\frac{\partial \tau_{xy}}{\partial x} + \frac{\partial \tau_{yy}}{\partial y} + \frac{\partial \tau_{zy}}{\partial z} \right) + \rho g$$

- **z- direction;**

$$\nabla . (\rho w V) = -\frac{\partial p}{\partial z} + \left(\frac{\partial \tau_{xz}}{\partial x} + \frac{\partial \tau_{yz}}{\partial y} + \frac{\partial \tau_{zz}}{\partial z} \right)$$

Energy equation,

$$\nabla . (\rho e V) = -p \nabla . V + \nabla . (k \nabla T) + \dot{q} + \varphi$$

For heat dissipationφ;

$$\varphi = \mu \left[2 \left[\left(\frac{\partial u}{\partial x} \right)^2 + \left(\frac{\partial v}{\partial y} \right)^2 + \left(\frac{\partial w}{\partial z} \right)^2 \right] \right] + \left(\frac{\partial u}{\partial y} + \frac{\partial v}{\partial x} \right)^2 + \left(\frac{\partial u}{\partial z} + \frac{\partial v}{\partial x} \right)^2 + \left(\frac{\partial v}{\partial z} + \frac{\partial w}{\partial y} \right)^2 + \lambda (\nabla . V)^2$$

Design

Using CATIA, the STHXs' three-dimensional geometries were generated. Taking into account a "shell-and-tube heat exchanger" with a set of circularly divided baffles that are 25% chopped. A 510 mm long shell with 50 mm equal diameters at the intake and outflow allows hot water with a temperature of 65°C to pass through it. Through a 520 mm tube bundle that is joined at both ends to the primary head of the outlet and the inlet diameter of 50 mm, cold water with a temperature of 10 °C flows. Total length of the shell and tube heat exchanger is 725 mm. Shell diameter of 140 mm represent by D1, tube inner and outer diameter of 16mm and 18 mm represent by D3, and D2 respectively. Other

dimension are represent in Figure 1(b), which is L1, L2, L3, L4 of 61 mm, 40.41mm, 20.21 mm, and 35 mm respectively. Figure 1(b) and Figure 2 show the various dimensional perspectives of the geometry. Figure 1(a) provides a more detailed view of the various STHX parts, including the ports and outlets of the tubes, the shells, and the baffles with alternating orientations. Figure 1(b) shows triangular tube layout patterns of the shell-and-tube heat exchanger. Two configuration of shell and tube heat exchanger has use in this study and in both configuration two different number of baffle are present. There are five and six baffle are present in design (configuration) 1 and 2 respectively, show in Figure 2. All other parameters including the number of tube bundles are same in both setups. Various distance illustrate in Figure 2 as L7 represent the thickness of the baffle, which is 4 mm, L5 is the distance between shell, and baffle, which is 83 mm. L8 and L6 represent the distance between each baffle, which is 64 mm, and 81 mm respectively.

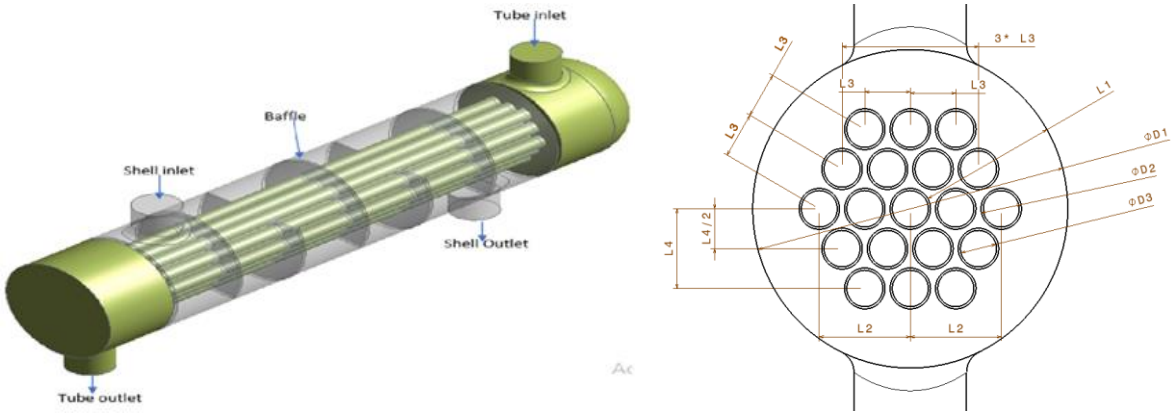

a. 3D Schematic diagram, b. Tube pattern dimension representation

Figure 1 Geometry of shell and tube representation

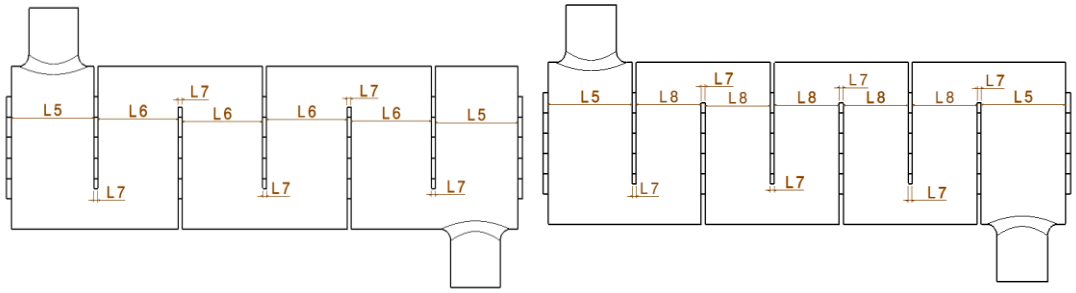

a. Configuration 1 – 5 baffle b. Configuration 2 – 6 baffle

Figure 2 Baffle representation in configuration 1 and 2

Mesh generation

Grid generation is crucial for achieving precise numerical results while reducing processing time. This mesh was created with the help of ANSYS Mesh. Considering the intricate geometry, the shell and tubes were modelled using an unstructured tetrahedral mesh with an element size of 0.001 for the tube domain and 0.02 m for the remainder domain, as seen in the picture. During the mesh generation element and nodes are form for configuration 1- 5 baffle it is 2,421,369 & 1,458,340 and for configuration 2- 6 baffle it is 2,414,989 & 1,457,692 respectively.

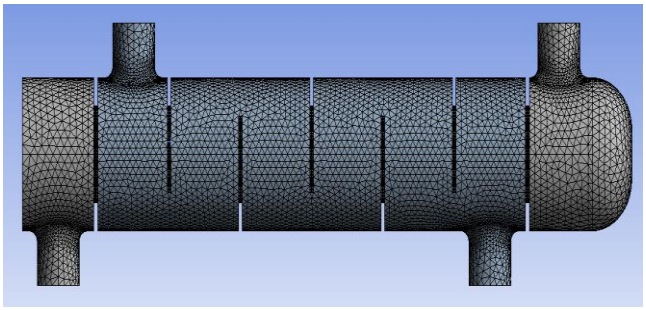

Figure 3 Mesh generation on shell and tube heat exchanger of all domain

Boundary condition

A combination of the 3D Navier-Stokes model, the energy equation, and the turbulent flow (k - e realisable) model was used to address the problem. The executable models used were k-epsilon realisable turbulence and a pressure-based solver. Utilising the SIMPLE approach, the pressure-velocity coupling was established. The discretisation methodology was configured to be linear square cell-based. For pressure, momentum, and energy, the second-order upwind scheme was used. Each problem was solved using the convergence criterion of 1× 〖10〗 ^(-7) independently. The fluid passing through the shell's intake is hot (65 °C) and moving at a mass flow rate of 0.5 kg/s; in contrast, the fluid passing through the tube's entrance is cool (10°C), as shown in Table 2. For the shell and tube outlets, a zero-pressure gauge (0 Pa) is taken into account. Assumption of an adiabatic condition for all exterior walls and a no-slip boundary; setting of a linked thermal condition at the shell-tube contact. With an average temperature of 37.5 °C, Table 1 displays the thermos-physical parameters of both hot and cold fluids. Assuming the three-dimensional, incompressible, turbulent, steady-state flow with heat transfer.

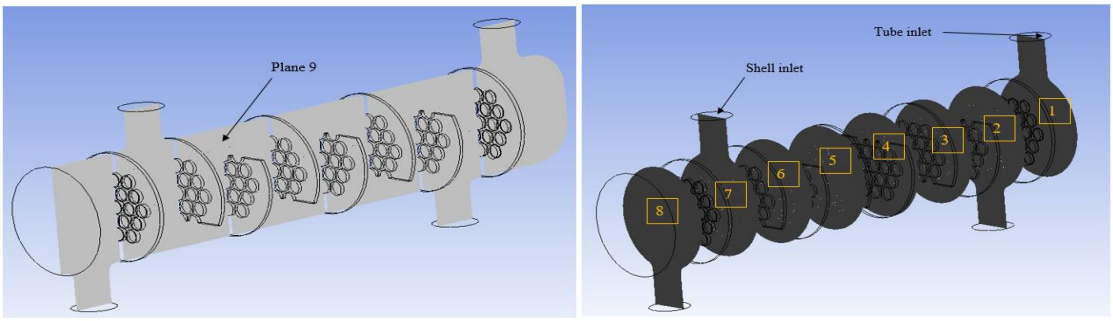

Figure 4 Plane representation

Table 1 Thermal properties of fluids and solid

Properties	Cold and hot water's thermal characteristics at the mean temperature (Tm = 37.5 °C)	Solid material (Steel)
Specific heat (Cp)	Hot water: 4186.5 J/kgK, Cold water: 4180 J/kgK	502.48 J/kgK D
Thermal conductivity (k)	0.6 W/mK	16.27 W/mK
Density (ρ)	998 kg/m3	8030 kg/m3
Dynamic viscosity (μ)	0.001003 kg/ms	

Table 2 Case natation with design and mass flow rate combination

Cases	Configuration	Mass flow rate (shell)	Mass flow rate (Tube)
Case 1 – 5 baffle	Design 1 (5 baffle)	0.5 kg/s	0.2 kg/s
Case 2 – 6 baffle	Design 2 (6 baffle)	0.5 kg/s	0.2 kg/s
Case 3 – 0.3S/0.2T	Design 2 (6 baffle)	0.3 kg/s	0.2 kg/s
Case 4 – 0.3S/0.15T	Design 2 (6 baffle)	0.3 kg/s	0.15 kg/s
Case 5 – 0.2S/0.1T	Design 2 (6 baffle)	0.2 kg/s	0.1 kg/s

Table 3 Plane distance

Planes	Distance (m)	Planes	Distance (m)
1	0.0845	5	0.4215
2	0.1675	6	0.5075
3	0.2525	7	0.5925
4	0.3375	8	0.6825

Validation

For validate the current simulation result obtained from the CFD with result obtained from (Fetuga et al., 2023) [17] simulation compare the outlet temperature of shell fluid and tube fluid. Consider a shell and tube heat exchanger of triangular tube layout with mass flow rate at shell and tube inlet of 0.5 and 0.2 kg/s respectively. Cold-water flow in the tube with 10 °C temperature and hot water flow in the shell side with 65 °C. Heat exchanger use for the validate have 5 baffle and other geometric parameter are present in design section and design show in the Figure 1 and Figure 2(a). ANSYS fluent use for the simulation. For turbulence flow K-ε realizable method select. Thermo-physical properties of fluid and solid use for simulation are present in Table 1. Validation result are show in the Figure 6 with a difference of 1.5 K, and 0.945 k of outlet temperature at shell side and tube side respectively.

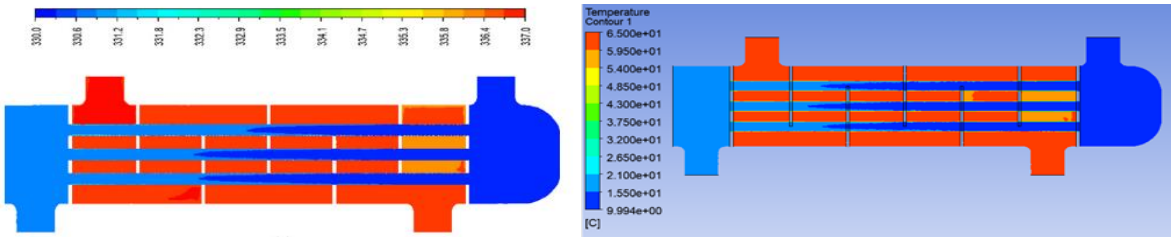

a. (Fetuga et al., 2023) **b. present study**

Figure 5 Temperature contour validation

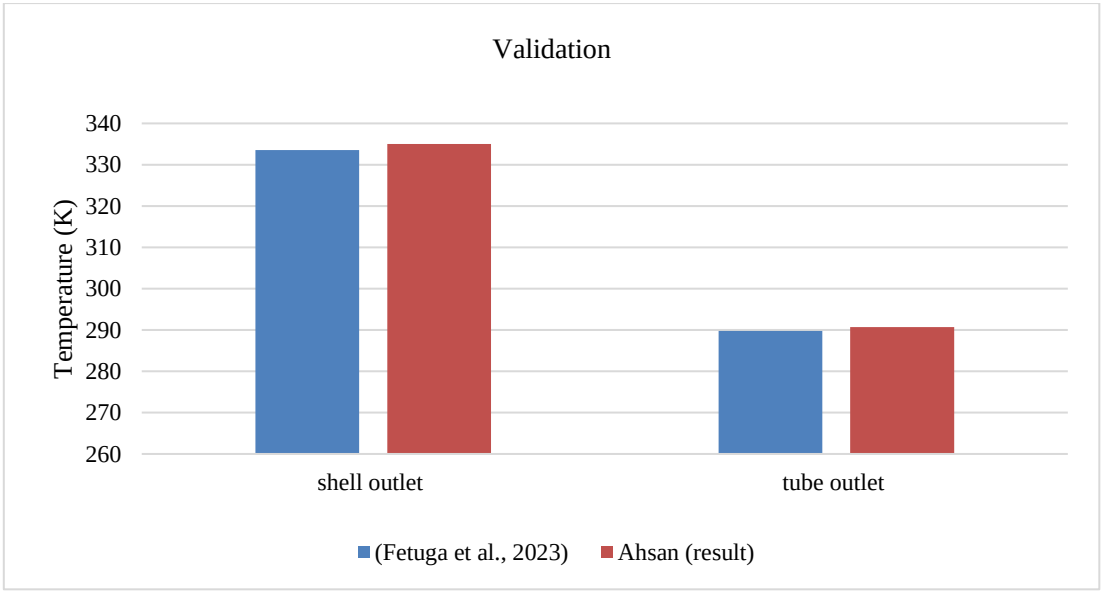

Figure 6 Validation result

RESULT AND DISCUSSION

Temperature contour due to baffle pattern

Figure 7 and Figure 8 illustrates the temperature variation on both configuration of baffle in the tube side and shell side with constant mass flow rate of 0.5 kg/s and 0.2 kg/s on the shell side and tube side respectively. Increases the outlet temperature of tube and decreases the outlet temperature of shell it happen due to increasing the baffle number. Due to increases baffle number, increases the number of passes of shell fluid to tube fluid. After that the contact area is increases between shell fluid and tube fluid due to that shell fluid temperature decreases and tube fluid temperature is increases. Figure 9 illustrate the value of outlet temperature of tube and shell.

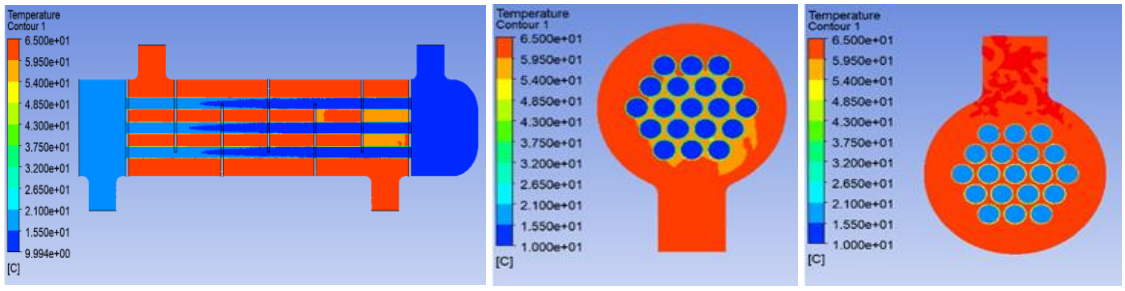

a. Plane 9 **b. Plane 2** **c. Plane 7**

Figure 7 Temperature contour of case 1 – 5 baffle

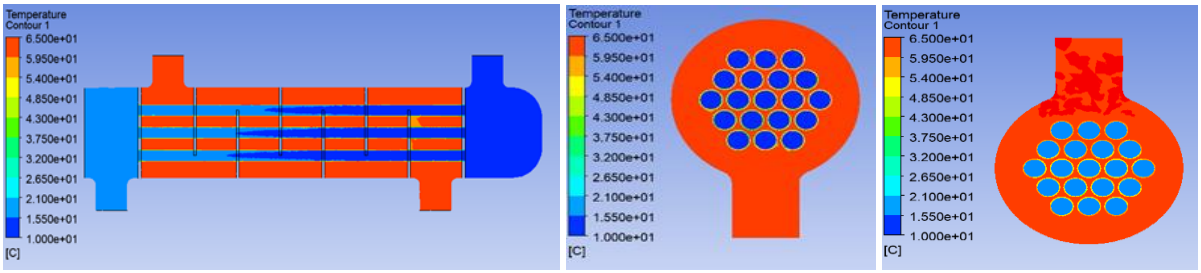

a. Plane 9 **b. Plane 2** **c. Plane 7**

Figure 8 Temperature contour of case 2 – 6 baffle

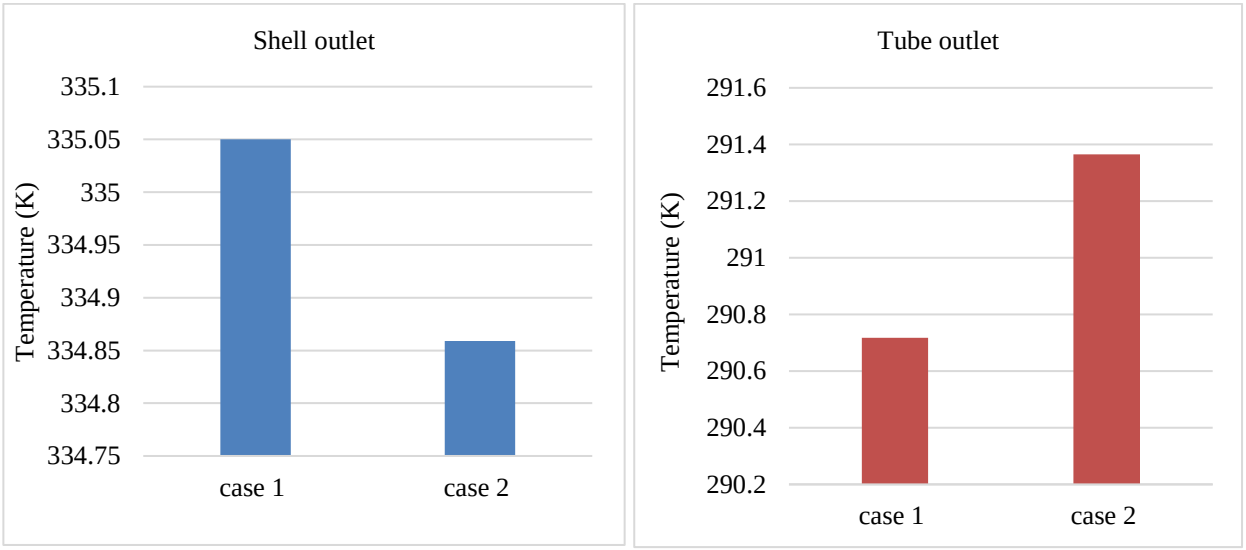

Figure 9 Outlet temperature at both shell and tube due to change in baffle

Temperature contour due to change in mass flow rate

Changes in the mass flow rate at the shell and tube input cause temperature variations, as seen in Figure 10, Figure 11, and Figure 12. In the inlet of shell two value of mass flow rate are select which are 0.3 and 0.2 kg/s. in the inlet of the tube three value of mass flow rate are select which are 0.2, 0.15, and 0.1 kg/s. The combination of mass flow rate of both inlet shell and tube are illustrate in Table 2. Case 3 shows that the shell's and tube's outlet temperatures are reduced when the mass flow rate of the shell inlet is decreased. In the case 4 the mass flow rate has constant as in case 3, decreases the temperature of tube inlet due to that combination increases the outlet of the both shell and tube. After that decreasing the mass flow rate of both shell and tube in case 5 resultant is reduction in outlet temperature of shell and increase in outlet temperature of tube. Value comparison of each cases of outlet temperature of shell and tube are illustrate in Figure 13.

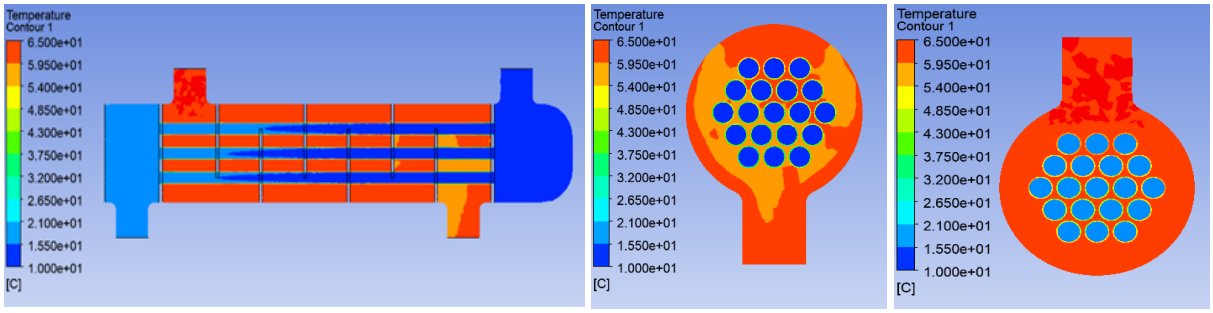

Figure 10 Temperature contour of case 3 – 0.3S/0.2T

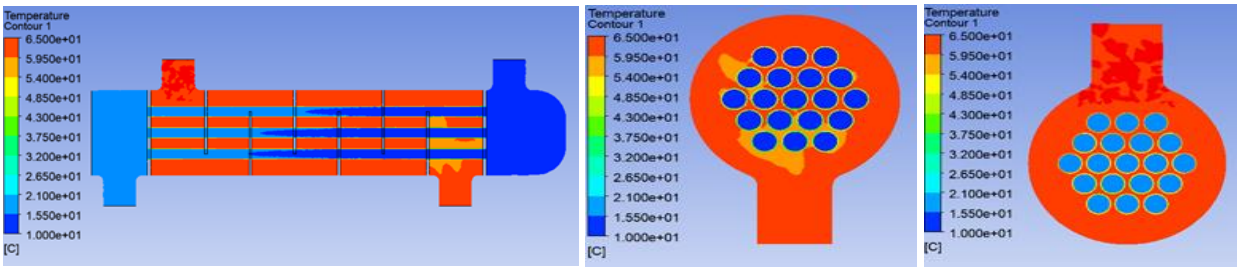

Figure 11 Temperature contour of case 4 – 0.3S/0.15T

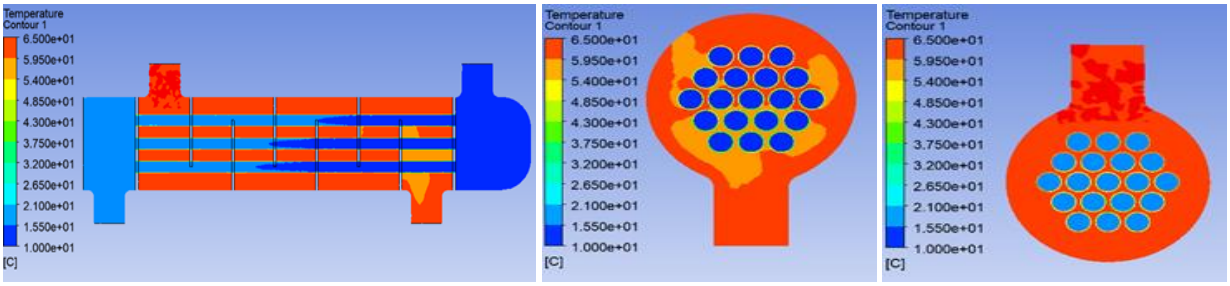

Figure 12 Temperature contour of case 5 – 0.2S/0.1T

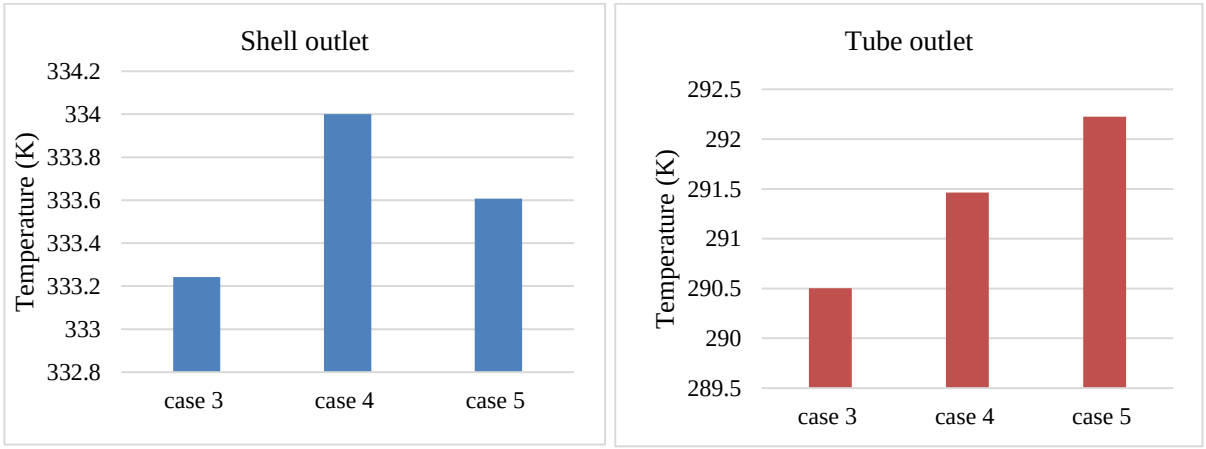

Figure 13 Outlet temperature at both shell and tube due to change in mass flow rate

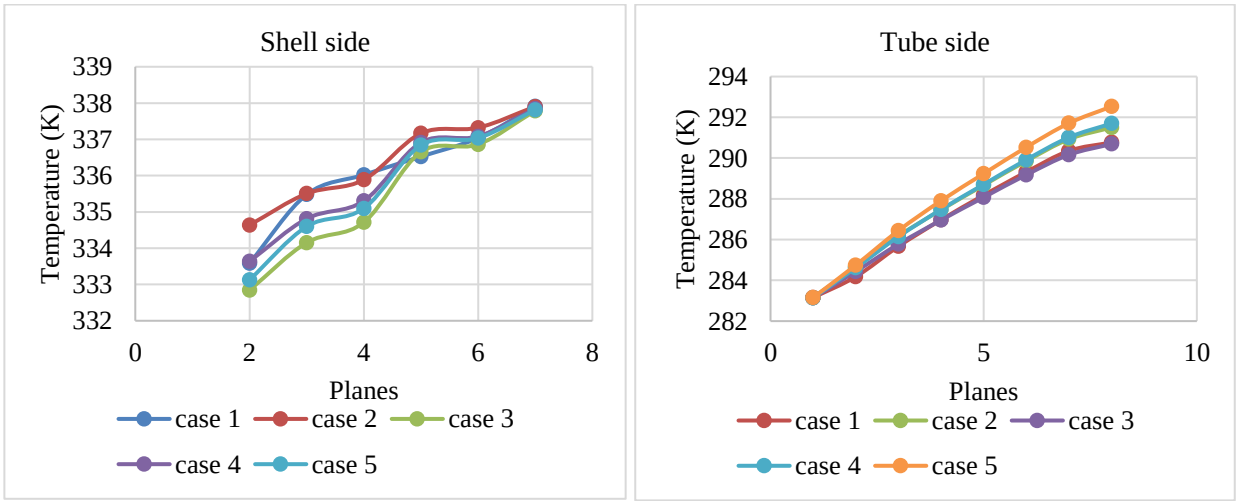

Figure 14 Average temperature in plane

Pressure contour

Pressure variation on the both tube and shell for each cases illustrated in Figure 15. Graph Figure 16 illustrate increase in pressure drop of shell side and decreases in pressure drop of tube side due to increasing in baffle numbers. In case 3, with the maximum baffle design, the pressure drop on both the shell and tube sides is lowered because the mass flow rate of the shell intake is reduced. In case 4, constant mass flow rate of shell inlet and decrease the mass flow rate of tube inlet due to that pressure drop is constant in shell side and reduce in tube side. In the case 5, decreases the mass flow rate of both shell and tube, deceases the pressure drop in both side shell and tube. For each scenario, the Figure 16 shows the value of the pressure drop on the shell and tube sides. The Figure 16 shows the pressure value in relation to the plane that runs the length of the shell and tube. According to graph in shell side and tube side value of pressure drop and along the length, case 5 having the lowest pressure and maximum pressure drop of shell and tube side in case 2 and case 1 respectively.

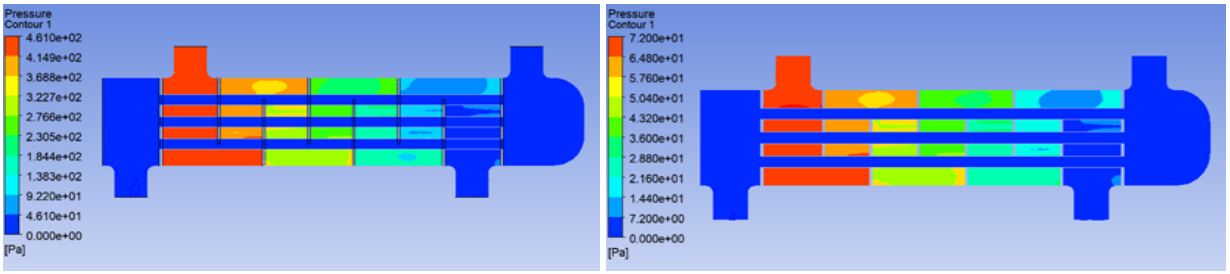

Case 2 **Case 5**

Figure 15 Pressure contour of each cases

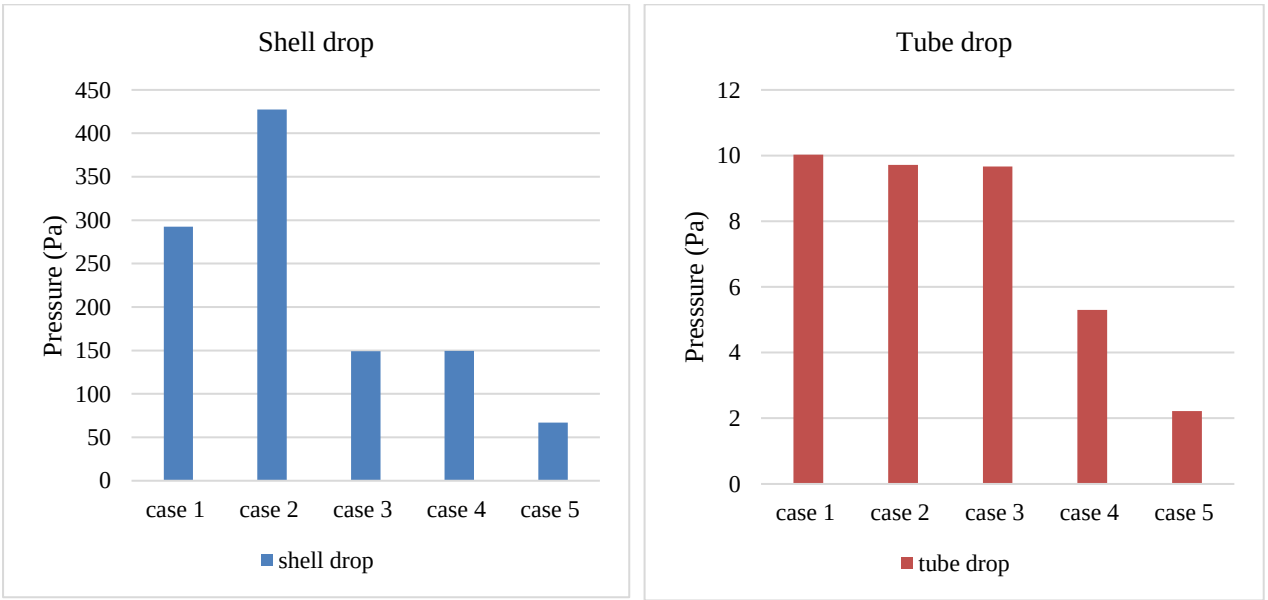

Figure 16 Pressure drop in each cases at tube and shell side

Velocity streamline

The fluid flow in the shell and tube sides of each instance is shown in the Figure 17. The distribution of velocity is uniform along the side of the tube. The baffle causes the velocity at the shell side to be uneven. In the case 1, lowest and highest value of velocity at plane 2 & Plan 7 in the shell and Plane 8 & Plane 1 in the tube side. In the shell side velocity follow uniformly pattern along the length illustrate in graph Figure 18. In case 2, 3, 4 and 5 having same value at plane 2 and plane 7 in each cases respectively in shell side. Also the maximum velocity at plane 5 in case 2, 3, 4, and 5 in shell side. In the comparison, case 5 having lowest velocity in all plane of each cases at shell side and tube side.

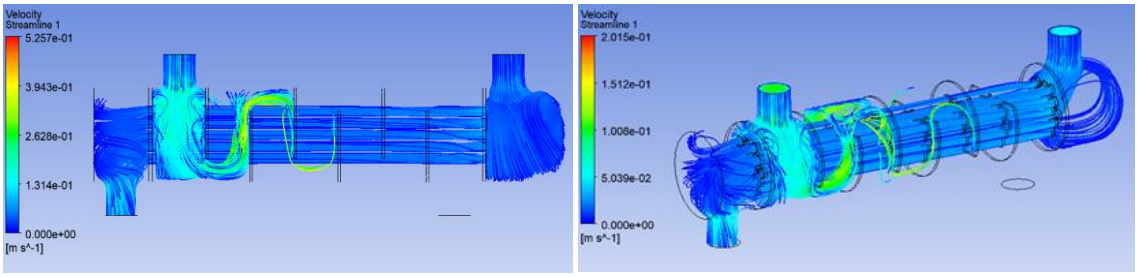

Case 2 **Case 5**

Figure 17 Velocity streamline of each cases

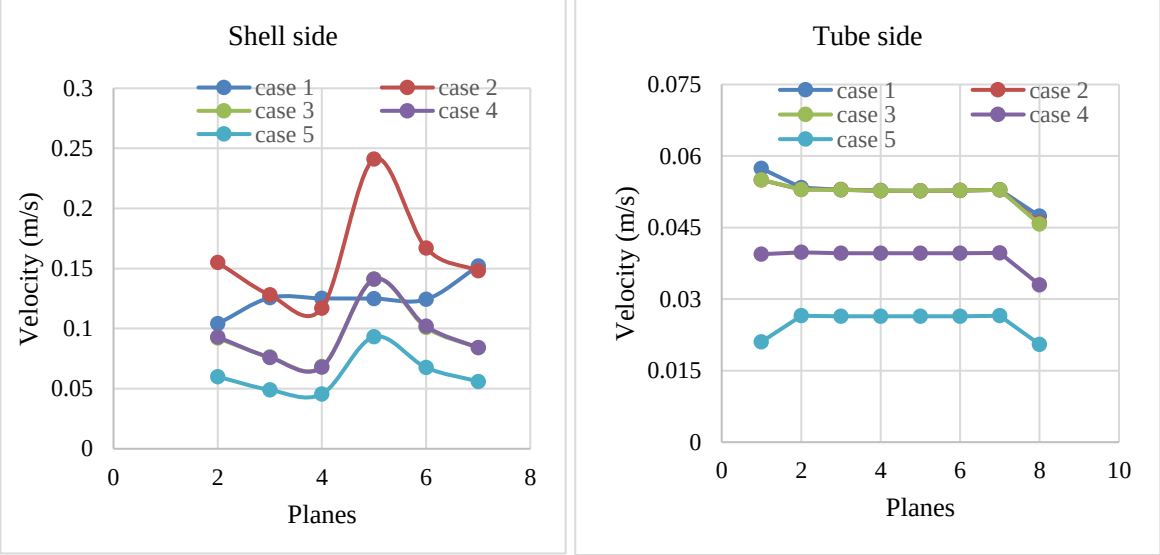

Figure 18 Average velocity at plane in tube and shell

CONCLUSION

A lot of waste heat recovery systems use custom-built and -operated heat exchangers to meet specific heat recovery needs. Nevertheless, the objective of this research is to address the need for heat recovery from a process that emits 65 °C effluent into the atmosphere. The study's primary objective is to find ways to make STHXs better "waste heat recovery systems" so that they can harness that heat for more profitable purposes. Computer-aided design (CFD) looked at the tube's heat transfer properties for a cold fluid flow. The sale transfers heat from one fluid to another by means of a flow of hot fluid. The transitional flow regime's features, including heat transmission and pressure decrease, are the primary emphasis.

- From the case 2, increasing the baffle number decreasing the shell outlet temperature and increases the tube outlet temperature.
- In the case 3, decreasing the mass flow rate of shell fluid resultant decreasing the shell and tube outlet temperature.
- In the case 4, the outlet temperatures of the shell and tube fluids are increased when the mass flow rates of the two fluids are kept constant while the mass flow rates of the tube fluid are decreased.
- In case 5, lowering the mass flow rate of the fluid in the shell and the tube led to a drop in the shell's outlet temperature and a rise in the tube's.

REFERENCE

[1] B. Wang, J. J. Klemeš, N. Li, M. Zeng, P. S. Varbanov, and Y. Liang, “Heat exchanger network retrofit with heat exchanger and material type selection: A review and a novel method,” Renew. Sustain. Energy Rev., vol. 138, no. September, 2021, doi: 10.1016/j.rser.2020.110479.

[2] T. N. Tien, Q. K. Vu, and V. N. Duy, “Novel designs of thermoelectric generator for automotive waste heat recovery: A review,” AIMS Energy, vol. 10, no. 4, pp. 922–942, 2022, doi: 10.3934/energy.2022042.

[3] S. Padhee, “Controller design for temperature control of heat exchanger system: Simulation studies,” WSEAS Trans. Syst. Control, vol. 9, no. 1, pp. 485–491, 2014.

[4] G. Colangelo, A. De Risi, and D. Laforgia, “New approaches to the design of the combustion system for thermophotovoltaic applications,” Semicond. Sci. Technol., vol. 18, no. 5, 2003, doi: 10.1088/0268-1242/18/5/318.

[5] J. Bonilla, A. de la Calle, M. M. Rodríguez-García, L. Roca, and L. Valenzuela, “Study on shell-and-tube heat exchanger models with different degree of complexity for process simulation and control design,” Appl. Therm. Eng., vol. 124, pp. 1425–1440, 2017, doi: 10.1016/j.applthermaleng.2017.06.129.

[6] E. C. Okonkwo, I. Wole-Osho, I. W. Almanassra, Y. M. Abdullatif, and T. Al-Ansari, An updated review of nanofluids in various heat transfer devices, vol. 145, no. 6. Springer International Publishing, 2021. doi: 10.1007/s10973-020-09760-2.

[7] E. Mokheimer and S. Said, “The Potential of Using Plate-and-Frame Heat Exchangers in Residential A/C Systems,” no. May, 2023, [Online]. Available: https://www.researchgate.net/publication/228904721_The_Potential_of_Using_Plate-and-Frame_Heat_Exchangers_in_Residential_AC_Systems

[8] M. J. H. Rawa, Y. A. Al-Turki, N. H. Abu-Hamdeh, and A. Alimoradi, “Multi-objective optimization of heat transfer through the various types of tube banks arrangements,” Alexandria Eng. J., vol. 60, no. 3, pp. 2905–2919, 2021, doi: 10.1016/j.aej.2021.01.017.

[9] M. A. M. Ali, W. M. El-Maghlany, Y. A. Eldrainy, and A. Attia, “Heat transfer enhancement of double pipe heat exchanger using rotating of variable eccentricity inner pipe,” Alexandria Eng. J., vol. 57, no. 4, pp. 3709–3725, 2018, doi: 10.1016/j.aej.2018.03.003.

[10] M. W. Tian, A. Abidi, S. R. Yan, D. Toghraie, and M. Degani, “Economic cost and efficiency analysis of the employment of inserting rods with helical fins in a shell and tube heat exchanger under magnetic field and filled with nanofluid,” Ain Shams Eng. J., vol. 13, no. 4, p. 101651, 2022, doi: 10.1016/j.asej.2021.11.020.

[11] H. Arjmandi, R. Amini, A. Ghaffari, H. Rahmani, and A. Chamkha, “Effects of baffles and vortex generators on cooling performance of a gas turbine combustion chamber: Numerical assessment,” Alexandria Eng. J., vol. 61, no. 6, pp. 4467–4478, 2022, doi: 10.1016/j.aej.2021.10.005.

[12] M. Klazly and G. Bognar, “Heat transfer enhancement for nanofluid flows over a microscale backward-facing step,” Alexandria Eng. J., vol. 61, no. 10, pp. 8161–8176, 2022, doi: 10.1016/j.aej.2022.01.008.

[13] M. Ben Slimene, S. Poncet, J. Bessrour, and F. Kallel, “Numerical investigation of the flow dynamics and heat transfer in a rectangular shell-and-tube heat exchanger,” Case Stud. Therm. Eng., vol. 32, no. December 2021, 2022, doi: 10.1016/j.csite.2022.101873.

[14] P. A. D. Cruz, E. J. E. Yamat, J. P. E. Nuqui, and A. N. Soriano, “Computational Fluid Dynamics (CFD) analysis of the heat transfer and fluid flow of copper (II) oxide-water nanofluid in a shell and tube heat exchanger,” Digit. Chem. Eng., vol. 3, no. September 2021, p. 100014, 2022, doi: 10.1016/j.dche.2022.100014.

[15] S. K. Gupta, H. Verma, and N. Yadav, “A review on recent development of nanofluid utilization in shell & tube heat exchanger for saving of energy,” Mater. Today Proc., vol. 54, no. October, pp. 579–589, 2022, doi: 10.1016/j.matpr.2021.09.455.

[16] N. Sinaga, S. khorasani, K. Sooppy Nisar, and A. Kaood, “Second law efficiency analysis of air injection into inner tube of double tube heat exchanger,” Alexandria Eng. J., vol. 60, no. 1, pp. 1465–1476, 2021, doi: 10.1016/j.aej.2020.10.064.

[17] I. A. Fetuga, O. T. Olakoyejo, S. M. Abolarin, J. K. Gbegudu, A. Onwuegbusi, and A. O. Adelaja, “Numerical analysis of thermal performance of waste heat recovery shell and tube heat exchangers on counter-flow with different tube configurations,” Alexandria Eng. J., vol. 64, pp. 859–875, 2023, doi: 10.1016/j.aej.2022.09.017.

[18] Kumar, K. et al. 2025. Examine the effect of various shape of absorber plate of solar air heater integrated with vortex generator. International Journal of Innovations in Science, Engineering And Management. 4, 1 (Jan. 2025), 118–129. DOI:https://doi.org/10.69968/ijisem.2025v4i1118-129.